ACS APPLIED MATERIALS & INTERFACES

Research Article

www.acsami.org

Poly(vinylidene fluoride)-Based Flexible and Lightweight Materials for Attenuating Microwave Radiations

Maya Sharma,[†] Mahander Pratap Singh,[‡] Chandan Srivastava,[‡] Giridhar Madras,[§] and Suryasarathi Bose*[,‡]

[†]Center for Nano Science and Engineering, [‡]Department of Materials Engineering, and [§]Department of Chemical Engineering, Indian Institute of Science, Bangalore 560012, India

ABSTRACT: Two unique materials were developed, like graphene oxide (GO) sheets covalently grafted on to barium titanate (BT) nanoparticles and cobalt nanowires (Co-NWs), to attenuate the electromagnetic (EM) radiations in poly(vinylidene fluoride) (PVDF)-based composites. The rationale behind using either a ferroelectric or a ferromagnetic material in combination with intrinsically conducting nanoparticles (multiwall carbon nanotubes, CNTs), is to induce both electrical and magnetic dipoles in the system. Two key properties, namely, enhanced dielectric constant and magnetic permeability, were determined. PVDF/BT−GO composites exhibited higher dielectric constant compared to PVDF/BT and PVDF/GO composites. Co-NWs, which were synthesized by electrodeposition, exhibited saturation magnetization (M_s) of 40 emu/g and coercivity (H_c) of 300 G. Three phase hybrid composites were prepared by mixing CNTs with either BT−GO or Co-NWs in PVDF by solution blending. These nanoparticles showed high electrical conductivity and significant attenuation of EM radiations both in the X-band and in the K_u-band frequency. In addition, BT−GO/CNT and Co-NWs/CNT particles also enhanced the thermal conductivity of PVDF by ca. 8.7- and 9.3-fold in striking contrast to neat PVDF. This study open new avenues to design flexible and lightweight electromagnetic interference shielding materials by careful selection of functional nanoparticles.

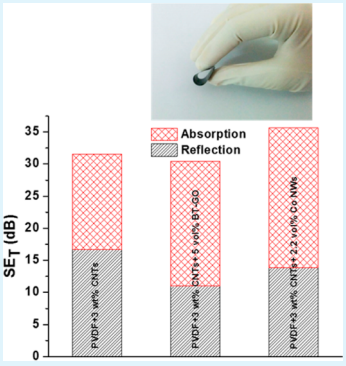

KEYWORDS: *poly(vinylidene fluoride), barium titanate, graphene oxide, cobalt nanowire, multiwall nanotubes, electromagnetic shielding*

INTRODUCTION

Because of the extensive use of electronic equipment, electromagnetic (EM) pollution has become common and this affects human health adversely and also the efficiency of the surrounding electronics[1,2] due to common impedance coupling.[3,4] Thus, the development of new materials that can absorb and/or reflect radiation has become necessary. The inclusion of conducting particles such as CNT (carbon nanotubes), CB (carbon black), metal fibers, and graphene in polymers can result in high electrical conductivity in the nanocomposites.[5−9] EM radiations consist of coupled electric and magnetic fields. Hence, materials with high electrical conductivity and high magnetic permeability are ideal. For instance, when electric field is applied to an electrically conducting material, the current that has been induced causes charge to displace which in turn cancels the applied field. Similarly, materials with high magnetic permeability provide an effective pathway for magnetic field, thereby shielding the EM radiations.

In this context, CNTs can be a promising material for shielding EM radiations due to its excellent electrical conductivity. Because of their one-dimensional structures, they can form a conducting path in the polymer matrix and can shield EM radiations effectively.[10−14] Further, functionalization of CNTs can help in their dispersion in polymer matrix,[15] thereby increasing the shielding efficiency. For example, we have recently reported enhanced electromagnetic interference (EMI) shielding in ionic liquid-modified CNTs in poly(vinylidene fluoride) (PVDF) matrix.[16]

In addition, materials with high dielectric constant and high dielectric loss can also shield EM radiations by absorption but unlike CNTs where the dominant mechanism is by reflection. In this regard, ferroelectric materials can be an ideal choice as losses in the ferroelectric phase are caused by electric hysteresis effects. Moreover, polymeric composites with a ferroelectric material can induce other losses like Maxwell−Wagner−Sillars polarization, capacitor effect, antenna effect, etc. In this context, $BaTiO_3$ has been widely studied for EMI shielding applications due to its high dielectric constant, positive temperature coefficient, and nonlinear optical properties.[17] For example, $BaTiO_3$ reinforced polyaniline composites showed shielding effectiveness of 25 dB at 11.2 GHz[18] while $BaTiO_3$ with Ag incorporated in PVDF matrix had a shield effectiveness of 26 dB.[19]

In addition, magnetic materials such as nickel, iron, and cobalt have also been studied for EMI applications. Nickel filaments in the poly(ether sulfone) matrix composites showed EMI shielding values up to 88 dB at 1−2 GHz.[20] Similarly,

Received: September 4, 2014
Accepted: November 10, 2014
Published: November 10, 2014

Scheme 1. Preparation of PVDF/CNT/BT−GO Composites

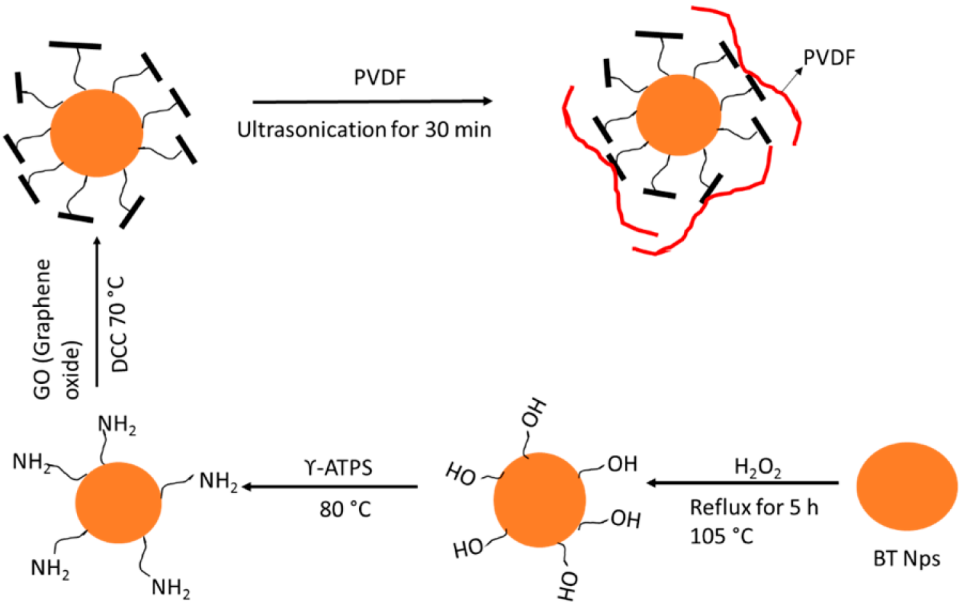

incorporation of 50 vol % carbonyl iron powder in the PVDF matrix increased the EMI shielding to 20 dB.[21] Fe−Al−Si alloy−polymer composite films showed excellent electromagnetic absorption in the microwave frequency range.[22] Feng et al.[23] reported flower-like FeNi@C nanocomposites with a thickness of 2 mm showed reflection loss of 46.7 dB at 3.17 GHz. Copper nanowires in the polystyrene matrix showed EMI shielding effectiveness of 42 dB at 13 wt % filler loading.[24] These studies open new avenues for developing metal-based polymer composites for controlling EMI pollution.

As mentioned, high electrical conductivity, high dielectric constant, and magnetic permeability are the key factors that decide the efficiency of a shielding material. Hence, we believe that a careful selection of materials can help in designing enhanced EMI shielding materials. In light of this, we employed a three-phase structure involving either a ferroelectric phase or a ferromagnetic phase in combination with an intrinsically conducting nanoparticle (CNTs) to design lightweight and flexible PVDF-based nanocomposites. It is envisaged that the dielectric constant of graphene can be tuned by varying the level of oxidation in the graphene interlayer. This can in turn help in accumulation of space charge. As mentioned earlier, materials with high dielectric constant and loss factors can attenuate the EM radiations efficiently; hence, graphene oxide (GO) was chemically grafted on to intrinsically high dielectric constant barium titanate (BT) nanoparticles to further enhance the dielectric constant of the nanocomposites. To enhance the magnetic permeability, cobalt nanowires (Co-NWs) were synthesized by electrodeposition and were used in combination with CNTs in PVDF. Electrical conductivity of the nanocomposites was evaluated using four-probe impedance spectroscopy and the EM shielding effectiveness was measured using a vector network analyzer.

EXPERIMENTAL SECTION

Synthesis of Barium Titanate−Graphene Oxide (BT−GO) Nanoparticles and Preparation of BT−GO/PVDF Composites. Nanometer-sized BT particles (ca. 100 nm) were procured from Sigma-Aldrich. A two-step process was employed for surface modification of BT particles with silane groups. In the first step, BT particles were ultrasonicated in the presence of H_2O_2 for 20 min. This mixture was further refluxed for 5 h at 105 °C to induce −OH functional groups on to the surface of BT particles. The resultant solution was centrifuged, washed repeatedly with deionized (DI) water, and dried at 80 °C for 12 h. In the second step, 200 mg of BT−OH nanoparticles was mixed with 10 mL of γ-aminopropyltriethoxysilane (APTS) and the resultant mixture was stirred at 80 °C for 24 h under N_2 atmosphere to yield BT−NH_2 nanoparticles. It is well-known that silane coupling agents, besides improving the dispersion,[25,26] also anchor on to OH-terminated nanoparticles. The BT− NH_2 nanoparticles were further dispersed in toluene and mixed with GO (synthesized by modified Hummer's method, as described elsewhere[27]) using a bath sonicator for 30 min in the presence of dicyclohexylcarbodiimide as a catalyst. The resultant solution was stirred for 24 h at 70 °C. GO-grafted BT nanoparticles were centrifuged and washed with commercial toluene to remove ungrafted GO particles. The samples were dried in a vacuum oven for 24 h at 80 °C (see Scheme 1). Solution casting method was employed for fabricating PVDF/BT−GO composites. Kynar PVDF 761 (from Arkema Inc., M_w 440 000 g/mol) was used as the matrix. Initially, PVDF was dissolved in *N*,*N*-dimethylformamide (DMF) and BT−GO (5 vol %) was added to this solution and mixed using a shear mixer at 8000 rpm for 45 min. The ceramic/polymer suspension was then poured into a Petri dish and left to dry.

Preparation of PVDF/CNT/BT−GO Composites. For fabricating PVDF/CNT/BT−GO composites, (3 wt %) amine-functionalized multiwall carbon nanotubes (CNTs, Nanocyl, Belgium) were dispersed in DMF using ultrasonication and was added to the polymer/ceramic suspension. The resultant solution was then subjected to shear mixing at 8000 rpm for 45 min followed by casting on to a Petri dish and left for drying at 80 °C under vacuum. Subsequently, PVDF/CNT/BT−GO films were obtained with a thickness of ca.100 mm and were used for additional experiments.

Preparation of PVDF/CNT Composites. PVDF was dissolved in DMF at 60 °C to form a clear solution. In another beaker, amine-functionalized CNTs (3 wt %) were dispersed in DMF using ultrasonication and mixed with the PVDF solution. The resultant mixture was then subjected to shear mixing as described above to yield a homogeneous mixture. A film was obtained as described above.

Synthesis of Cobalt Nanowires and Preparation of PVDF/CNT/Co-NWs Composites. Cobalt nanowires (Co-NWs) were synthesized using electrodeposition (Scheme 2). To achieve the nanowire morphology, alumina templates (anodic) containing cylindrical pores of 200 nm diameter and 60 μm length were used.

Scheme 2. Various Elements Involved in Electrodeposition of Cobalt Nanowires

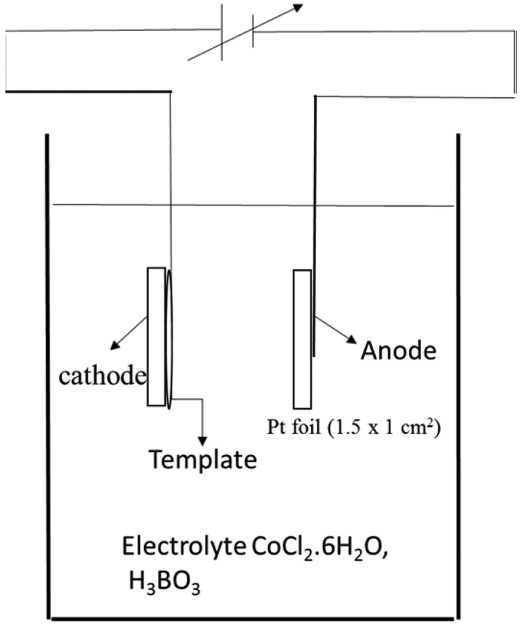

The alumina template was attached to a copper foil through a conductive tape. This assembly was used as the cathode. Pt foil (1.5 × 1 cm^2) was used as the anode. Before electrodeposition, the cathode was kept in DI water for 4 h to release the entrapped air from within the pores, which further increases the efficiency of the deposition process. The electrolyte for the deposition was prepared by dissolving extra pure cobalt chloride hexahydrate ($CoCl_2 \cdot 6H_2O$, 4.579 g) and boric acid (H_3BO_3, 4.579 g) in 150 mL of DI water. The interelectrode distance was 2.5 cm. Electrodeposition was carried out at a constant current of 14 mA for 2 h at 25 °C under argon. After the electrodeposition, the anodic-containing nanowires were kept immersed in 1 M NaOH solution for 3 h to dissolve away the alumina template. Co-NWs released from the host matrix were centrifuged and washed repeatedly in DI water for further characterization.

Co-NWs (2.2 vol %) were dispersed in DMF using ultrasonication for 20 min to form a stable suspension. Ultrasonication was done at low amplitude to prevent the breakage of Co-NWs. Suspension of Co-NWs was then added to PVDF/CNT solution (as described above) and subjected to a shear mixer under the same conditions, as described above. This mixture was then poured onto a Petri dish and left to dry.

Characterization of the Nanoparticles. For assessment of the covalent grafting of GO sheets on to BT nanoparticles, X-ray photon scattering (XPS, Kratos Analytical instrument) spectra were obtained using an Al monochromatic source (1.486 keV). FTIR scans (Perkin-Elmer) were done to ensure the completion of reaction at each step. The morphology of the as-prepared Co-NWs was evaluated by ESEM Quanta scanning electron microscopy. X-ray diffraction (XRD) scans were recorded using a PANalytical X'pert Pro using Cu Kα radiation. A vibrating sample magnetometer (LakeShore) was employed for measuring the magnetic properties of the nanowires at room temperature using a field of 2 T.

Characterization of Composites. Alternating current electrical conductivity was measured on hot-pressed discs of 10 mm diameter in a broad frequency range of 10^{-1} to 10^7 Hz using an Alpha-N analyzer (Novocontrol). Sample electrodes were prepared by coating with silver paste on both the sides to provide good contact with the electrodes. For EMI measurements, An Anritsu MS4642A vector network analyzer with coax setup (Damaskos M 07T) was employed. The scattering parameters were measured in the X- and the K_u-band frequency limits. A full two-port short open load test (SOLT) calibration of the setup was done prior to sample measurements.

RESULTS AND DISCUSSION

Covalent Grafting of GO Sheets on to BT Nanoparticles. The grafting of GO onto BT was confirmed using XPS (see Figure 1a–f). The peaks were deconvoluted using curve-fitting software. Six elements—Ba, Ti, C, O, N, and Si—were obtained on the surface of BT–GO nanoparticles as evident from the wide spectrum of BT–GO nanoparticles (see Figure 1a). The C 1s spectrum of GO is shown in Figure1b, and the binding energies of the C–OH, C═O, and O═C–OH functional groups of graphene oxide are assigned to 285.5, 287.7, and 289.1 eV, respectively. The C 1s spectra of BT–GO given in Figure 1c have two prominent peaks: one at 285.7 and another at 289 eV, which can be fitted to C–OH and O═C–OH functional groups of graphene oxide on the BT–GO surface, respectively. The presence of free C–OH and O═C–OH groups on the BT–GO surface confirms the grafting of GO on the BT surface. The 287.7 eV peak is not visible in the BT–GO spectra. Figure 1d shows the N 1s spectra for BT–GO. The peak can be deconvoluted into two peaks, wherein the peak at low binding energy (400.9 eV) corresponds to the free terminal $-NH_2$ and the peak at high binding energy (403.9 eV) can be attributed to nitrogen from the amide linkage (−CONH). The presence of free amine functional groups on the BT nanoparticles indicate that only a few amine groups were utilized in the grafting process. The O 1s spectra analysis shown in Figure 1e,f can complement the C 1s spectra. The O 1s peak at 533 eV is assigned to the contribution from the C–OH groups on GO present on the BT–GO nanoparticle (Figure 1f). These observations further confirm the grafting of GO onto BT nanoparticles.

Figure 2 compares the spectra of BT bulk, BT–OH, BT–NH_2, and BT–GO particles. In BT–OH, the peak at 3400 cm^{-1} denotes the presence of oxygen moieties on the particles, which is absent in BT particles. The particles were modified with APTS, as described in the Experimental Section, and these particles are denoted as BT–NH_2 in which the peak at 1250 cm^{-1} represents the Si–O–Si vibration modes. The peak at 1570 cm^{-1} corresponds to the NH_2 scissoring vibration, thereby confirming the presence of silane molecules on the BT surface. The C–C stretching peak at 3300 cm^{-1} further confirms the presence of carbon on the surface of BT. FTIR spectra of BT–GO show apparent characteristic peaks at 3400 cm^{-1} (−OH), 1050 cm^{-1} (C–O), suggesting that graphene oxide has been successfully grafted onto BT particles.

As described earlier, one of the key requirements to attenuate EM radiations is high dielectric constant. It is well-known that BT particles show high dielectric constant at room temperature. We expect that by grafting of GO sheets on to BT nanoparticles, the charge can be attenuated. To gain more insight, the dielectric constant was measured using an impedance analyzer. The variation in the dielectric constant (ε') of neat PVDF, PVDF–BT (5 vol %), PVDF–GO (0.1 wt %), and PVDF/BT–GO (5 vol %) composites as a function of frequency is shown in Figure 3. The dielectric constant of PVDF increases with the addition of both BT nanoparticles and GO sheets. More interestingly, BT–GO nanoparticles exhibited a significant increase in the dielectric constant, manifesting in a synergistic improvement from both BT and GO sheets. The increase in the dielectric constant of PVDF with addition of three-phase structure is due to the large dielectric permittivity difference between the PVDF matrix and the particles (BT and GO), which causes the accumulation of

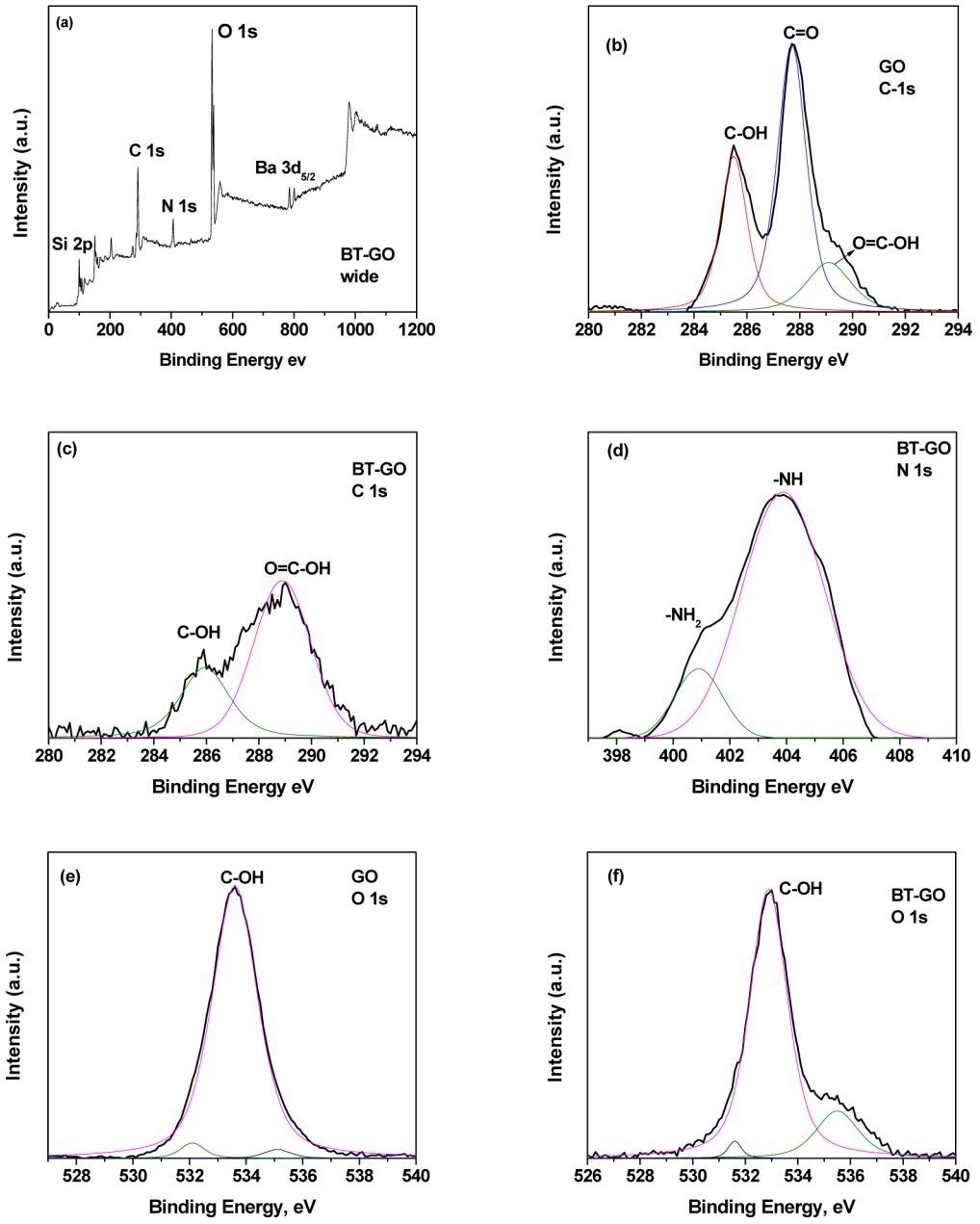

Figure 1. XPS spectra of nanoparticles: (a) wide spectra of BT−GO, (b) C 1s spectra of GO, (c) C 1s spectra of BT−GO, (d) N 1s spectra of BT−GO, (e) O 1s spectra of GO, and (f) O 1s spectra of BT−GO.

charge carriers at the interface. Similar results were reported earlier. For instance, Li et al. reported high dielectric permittivity and enhanced thermal properties in three-phase PVDF, BT, and silicon carbide nanocomposites.[28]

Morphology and Ferromagnetic Properties of Co-NWs. The morphology of the as-synthesized Co-NWs is shown in Figure 4a,b. It is very evident from Figure 4a that the adopted electrodeposition has resulted in a significant yield of nanowires. Scanning electron microscopy (SEM) micrograph of the cobalt nanowires revealed that the nanowires are approximately 200 nm in diameter and 55 μm in length which is expectedly the same as the pore size of the template. The XRD pattern of the as-synthesized cobalt nanowires array is shown in Figure 5. A high-intensity diffraction peak of hexagonally close packed cobalt phase is observed corresponding to the (0002) planes.[29,30]

Magnetic hysteresis was obtained from the as-synthesized nanowires at room temperature using a magnetic field of 2 T and is shown in Figure 6. The hysteresis loop was measured with the applied magnetic field parallel and perpendicular to the long axis of the nanowires. Nanowires showed ferromagnetic behavior with a saturation magnetization (M_s) of 40 emu/g and coercivity (H_c) of 300 G.

Electrical Conductivity and EMI Shielding of the Nanocomposites. The electrical conductivity of the PVDF/CNTs composites as a function of frequency is studied before exploring the effect of three-phase structures. The room-temperature electrical conductivities for various PVDF/CNTs composites are illustrated in Figure 7a,b. It is evident from Figure 7a that the conductivity increases with increasing concentration of CNTs in the PVDF matrix. While neat PVDF is insulating, the conductivity increased to 10^{-6} S/cm with the

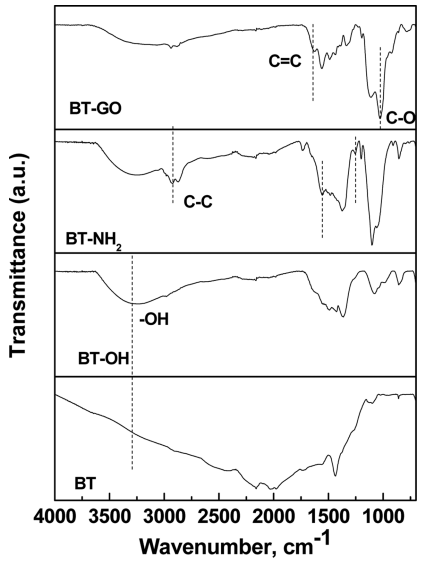

Figure 2. FTIR spectra of BT, BT−OH, BT−NH_2, and BT−GO.

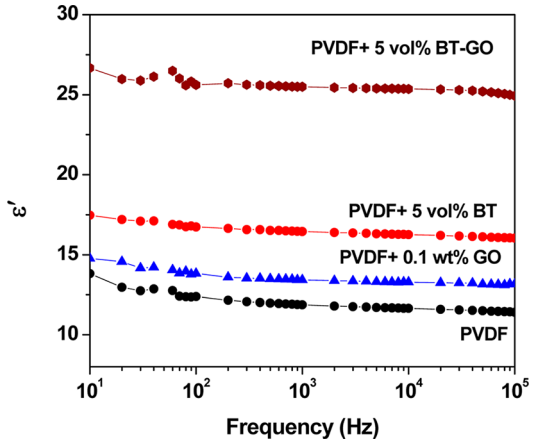

Figure 3. Variation of dielectric constants as a function of frequency for PVDF composites (with BT and GO).

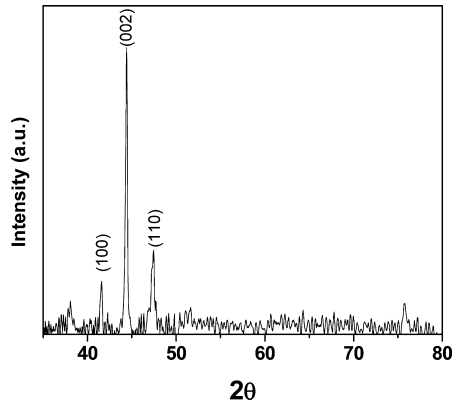

Figure 5. XRD of pure cobalt nanowires.

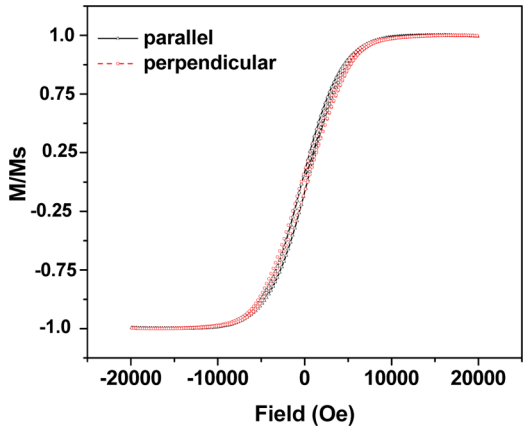

Figure 6. Normalized B−H curve, showing magnetization parallel and perpendicular to the wires.

addition of 1 wt % CNTs. As the concentration of CNTs increases, a dc plateau is observed in the low-frequency regime which increases with increasing frequency in the high-frequency regime (>10^6 Hz). PVDF/CNT composites with 3 wt % CNTs showed a conductivity of 10^{-3} S/cm, manifesting the formation of a conducting pathway in the PVDF matrix. The dc

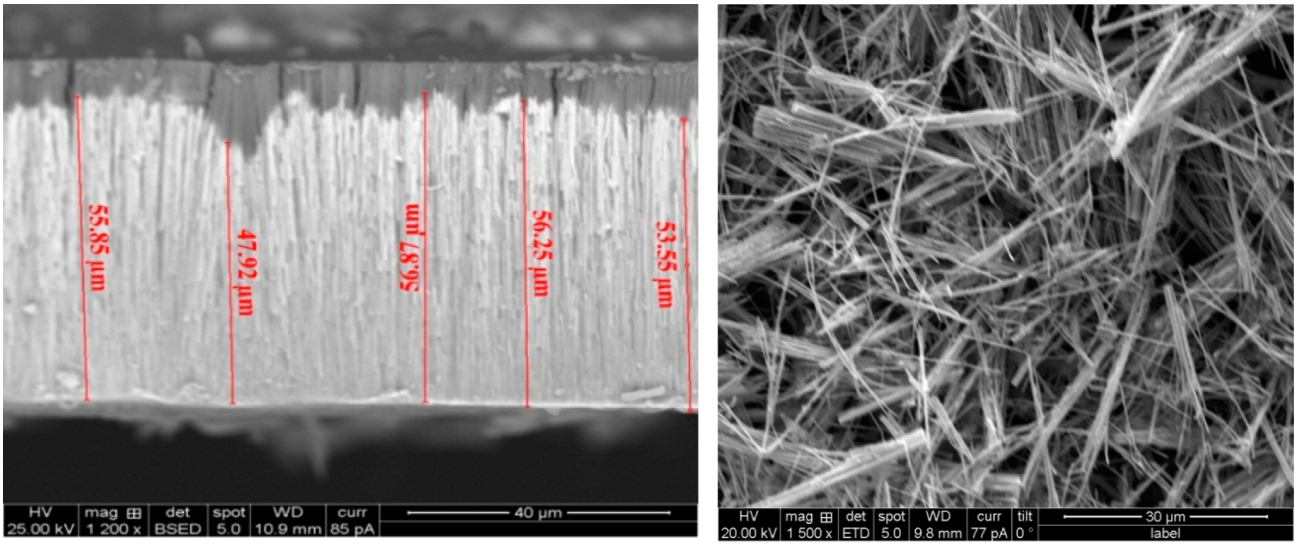

Figure 4. SEM image of cobalt nanowires: (a) cross-sectional image of template with wires; (b) dispersed nanowires on Si substrate.

dx.doi.org/10.1021/am506042a | ACS Appl. Mater. Interfaces 2014, 6, 21151−21160

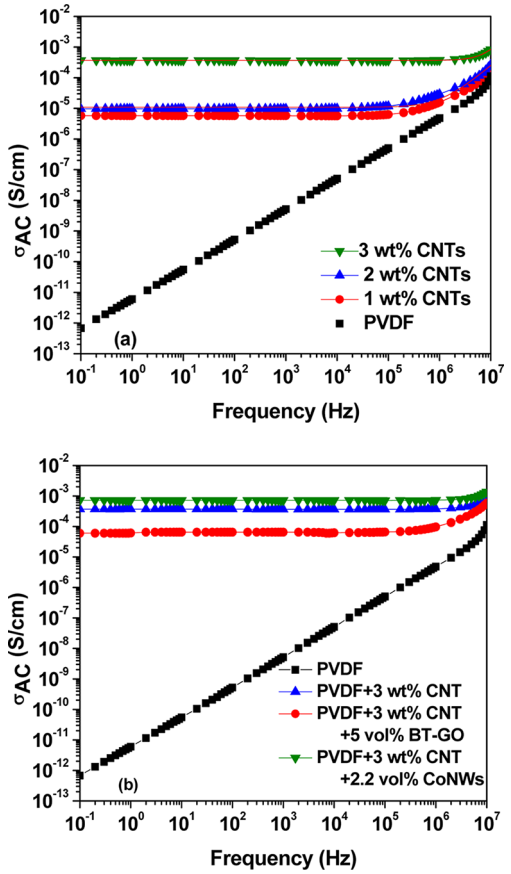

Figure 7. Electrical conductivity of (a) PVDF composites with different concentrations of CNTs and (b) PVDF composites with different nanoparticles.

conductivity of the nanocomposites with percolation threshold can be best explained using a power law[31,32] given by eq 1,

$$\sigma_{dc} \propto (p - p_c)^s \quad (1)$$

σ_{dc} represents the dc conductivity, p is the filler content, p_c is the electrical percolation threshold, and s is the exponent value.

The charge-transport mechanism in the composites can be explained using the ac universality law expressed as[33,34]

$$\sigma_{ac}(\omega) = \sigma_{dc}(\omega) + A(\omega)^s \quad (2)$$

In eq 2, σ_{dc} is the dc conductivity at $\omega \rightarrow 0$, the symbols A and s are temperature and frequency dependent parameters, and ω is the angular frequency.

Figure 7a,b shows that, above a certain point, the conductivity increases linearly with frequency. Thus, the dc contribution is important at low frequencies, whereas the frequency dependent parameter (s) dominates at high frequencies. The value of s was determined from the slope of the plot of $\ln(\sigma)$ versus $\ln(f)$ and this value can be used to explain the conduction mechanism operative in the sample. The value of s is ca. 0.9 for PVDF/CNT composites with 1 and 2 wt % CNTs, suggesting hopping of electrons. Further, the value of s as 0.6 for PVDF/CNT composites with 3 wt % CNTs suggests tunneling of electrons in the composites (Figure 7a). As mentioned earlier, two key properties were targeted in this study, high dielectric constant and high permeability. Hence, BT−GO and Co-NWs were synthesized. It is important to assess the effect of these nanoparticles on the electrical conductivity of PVDF/CNT composites. Few composites involving 2.2 vol % Co-NWs or 5 vol % BT−GO nanoparticles in combination with 3 wt % CNTs were prepared under the same mixing conditions. The conductivity of three-phase PVDF composites is illustrated in Figure 7b which shows that the addition of Co-NWs (10^{-3} S/cm) or BT−GO (6×10^{-5} S/cm) does not significantly alter the electrical conductivity of the composites. It is important to note that slightly reduced electrical conductivity in PVDF/BT−GO/CNT composites may be due to the addition of insulating BT−GO particles that hinders the charge transport through CNT network.

EMI shielding is a material property that can attenuate electromagnetic waves.[35] This can be either by reflection or by absorption. Thus, higher conducting materials have low impedance and, therefore, are successful at reflecting back electrically dominant waves because of the impedance mismatch. However, magnetically dominant waves have low impedance and absorption plays an important role in EMI shielding. Various mechanisms of shielding are illustrated in Scheme 3. For better EMI shielding, the material should

Scheme 3. Mechanism of EMI Shielding through Sample

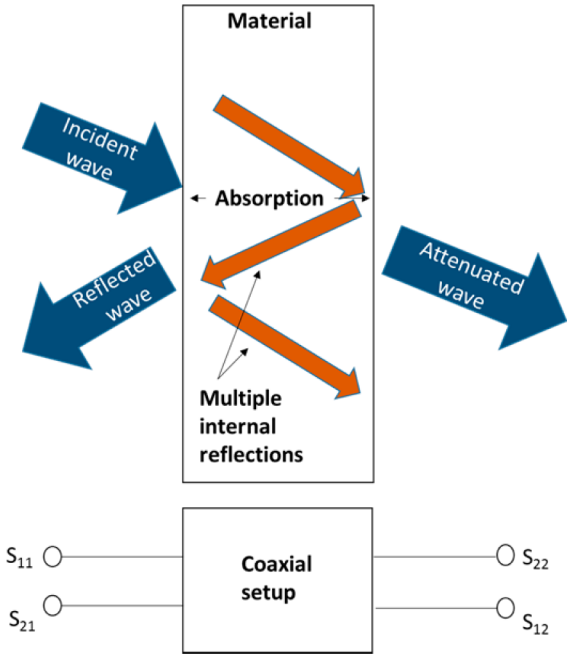

minimally reflect the incident EM wave and maximally attenuate the transmitted EM wave. Total shield effectiveness SE_T, reflection SE_r, and absorption SE_a can be calculated by using the scattering parameters S as given in eqs 3−5:

$$SE_R(\text{shield effectiveness} - \text{reflection}) = 10 \log_{10}(1/(1 - [S_{11}]^2)) \quad (3)$$

$$SE_A(\text{shield effectiveness} - \text{absorption}) = 10 \log_{10}((1 - [S_{11}]^2)/[S_{12}]^2) \quad (4)$$

$$SE_T(\text{shield effectiveness} - \text{total}) = SE_R + SE_A = 10 \log(1/[S_{12}]^2) \quad (5)$$

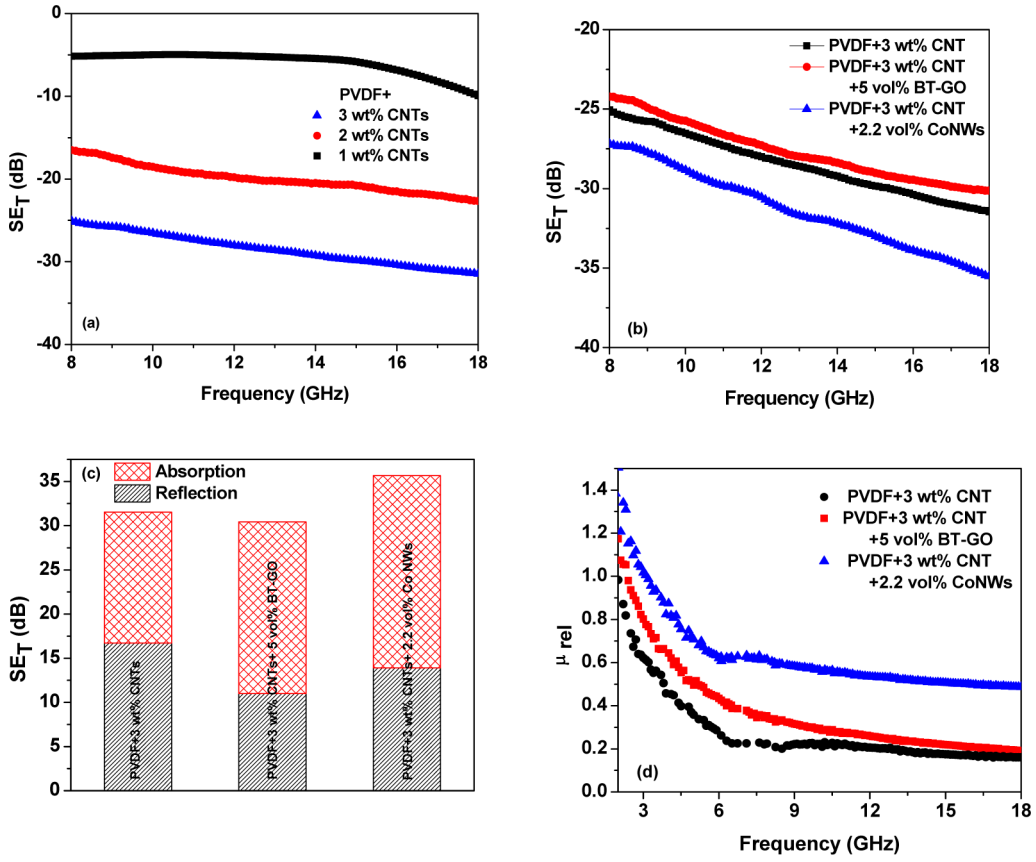

Figure 8. (a) Shield effectiveness of PVDF composites with different concentrations of CNTs, (b) shield effectiveness of PVDF composites with different nanoparticles, (c) comparison of absorption and reflection in PVDF composites with different nanoparticles, and (d) magnetic permeability of PVDF composites with different nanoparticles.

The EMI shielding effectiveness of PVDF/CNT composites with various concentrations of CNTs in X band and K_u band is depicted in Figure 8a. The shield effectiveness (SE) of the neat PVDF is almost zero as it is insulating in nature and is transparent to the EM radiations.[14,17] It is well evident that the effective shielding improves with increasing concentration of CNTs in the composites. For instance, PVDF with 1 wt % CNTs shows a SE of ca. 10 dB whereas with 2 wt % CNTs the SE reaches ca. 23 dB. The maximum SE of 31 dB was obtained with 3 wt % CNTs. This clearly indicates that SE increases with CNTs content and can be attributed to the interconnected network, resulting in better interaction between material and EM waves that block the EM interference.[36] The reflection and absorption contribution of SE was calculated using eqs 4 and 5 and it is well evident that in PVDF/CNT-based composites the reflection dominates over absorption.[36]

The EMI shielding of PVDF/BT−GO (5 vol %) is about 8 dB (not shown here) which clearly indicates that electrical conductivity is a key requirement to attenuate EM radiations. In composites involving 3 wt % CNTs and 5 vol % BT−GO in PVDF matrix, the total SE is though similar to PVDF with 3 wt % CNTs composites (shown in Figure 8b) but interestingly, the absorption component enhanced significantly. Figure 8c illustrates the absorption and reflection components of the total SE of composites. It is well evident that the absorption improves with addition of BT−GO in PVDF/CNT composites. For instance, in PVDF/CNT/BT−GO, the % absorption is ca. 63% which is significantly higher than the PVDF/CNT composites.

Interestingly, the EMI shield effectiveness of 35 dB was obtained with Co-NWs in combination with CNTs. This significant improvement in EMI shielding is due to a combined effect of cobalt nanowires and CNTs. The frequency dependence of SE for cobalt nanowires-based composite is shown in Figure 8b. The mechanism of EMI shielding is important in the application of shielding material. Figure 8c compares the reflection and absorption component of the SE in the PVDF/CNTs, PVDF/CNTs/BT−GO, and PVDF/CNT/Co-NWs.

For high reflections, the shield is required to have mobile charge carriers that interact with irradiated EM waves. But for absorption, the shield should have electric and/or magnetic dipoles that interact with the electromagnetic fields in the radiation. The electric dipoles may be provided by materials that have a high value of dielectric constant. The magnetic dipoles may be provided by materials having a high value of the permeability (μ).

It is interesting to note that the reflection and absorption components are almost similar in the PVDF/CNT composite which essentially means that CNTs-based composites can shield by both means: reflection and absorption. In the BT−GO-based composites, absorption is significantly higher than reflection which might be due to high dielectric constant of BT−GO nanoparticles which attenuate the EM waves. In the Co-NWs-based composites, absorption is observed to be the dominant mechanism. This increase in absorption is mainly due to the presence of magnetic nanowires which provides both magnetic as well as electrical shielding in the composites. This

Table 1. Examples of EMI Data Using Various Polymer Blends

matrix	filler	filler conc.	σ (S/cm)	SE (dB)	frequency (GHz)	references
PVDF	5 wt % MnO_2 NTs/1 wt % f-MWCNTs/PVDF		0.001	21	8−12	37
PVDF	activated carbon fibers	40 wt %	0.14	12−14	0.1−1	38
PVDF	copper NPs	35.8 wt %		40		39
PVDF	carbonyl iron powder	50 vol %	0.12	20	8−12	21
PVDF	barium titanate NPs	40 vol %	2.5×10^{-6}	9	8−12	19
	10 vol % Ag, 20 vol % BTn		0.01	26		
PVDF foam	functionalized graphene	5 wt %	0.01	20	8−12	36
PVDF	nickel and hexagonal-ferrite powders	50 vol %		67	8−12	40
PVDF	CNT/Co-NWs	3 wt % + 2.2 vol %	0.001	35	8−18	this work

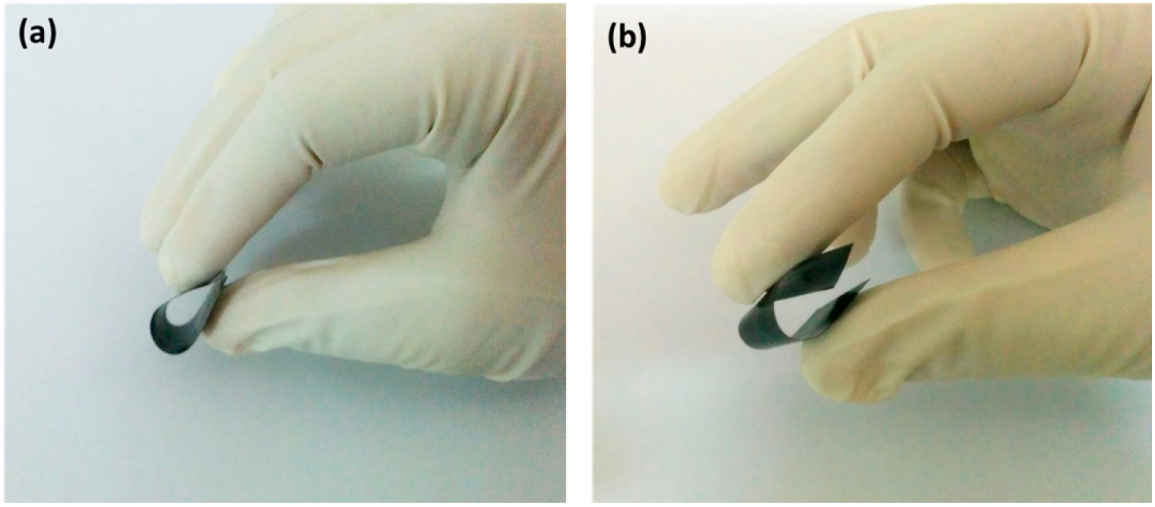

Figure 9. Flexible PVDF composites: (a) PVDF with 3 wt % CNTs + BT−GO nanoparticles and (b) PVDF with 3 wt % CNTs + Co-NWs.

is also well-supported by the observed permeability in the composites wherein PVDF/CNT/Co-NWs exhibit the highest permeability among the three composites. The magnetic permeability was calculated using the transmission line theory (see Figure 8d) which clearly indicates that a composite with cobalt nanowires shows maximum permeability among all the composites investigated here. More importantly, the SE obtained in this study is quite high given the concentration of the nanoparticles are quite low. To get a clear idea, Table 1 compares the electrical conductivity and SE of various PVDF-based composites. The results shown here clearly indicate that a careful selection of functionalized nanoparticles can facilitate tuning the SE in the composites.

Thermal Conductivity of the Composites. The current flowing through the active and passive components can result in power dissipation and increased temperatures. Therefore, a good electronic packaging material, apart from shielding external EM waves, should sustain the rise in temperature without any structural distortion. The thermal conductivity values for PVDF/CNT/BT−GO and PVDF/CNT/Co-NWs is not reported in the literature. The thermal conductivity of neat PVDF polymer is 0.19 W m^{-1} K^{-1}.[41] Different nanoparticles have been used to improve thermal conductivity of polymers. High-density polyethylene filled with 7 vol % expanded graphite has thermal conductivity of 1.59 W m^{-1} K^{-1},[42] poly(vinyl butyral), polystyrene, poly(methyl methacrylate), and poly(ethylene vinyl alcohol) based nanocomposites with 24 wt % boron nitride nanotubes have thermal conductivities of 1.80, 3.61, 3.16, and 2.50 W m^{-1} K^{-1}, respectively.[43] Carbon nanotubes was also reported to improve thermal conductivity of polymer composites.[44,45] PVDF/CNTs composites show a thermal conductivity of 2.66 W m^{-1} K^{-1}at 6.1 wt % of CNTs loading.[46]

PVDF with 3 wt % CNTs exhibited a thermal conductivity of ca. 1.68 W m^{-1} K^{-1}, which is significantly higher than the neat PVDF (0.3 W m^{-1} K^{-1}). On the other hand, PVDF/CNT/BT−GO showed even higher thermal conductivity (ca. 2.6 W m^{-1} K^{-1}) in striking contrast to PVDF/CNT composites. This increase in thermal conductivity with addition of BT is possibly due to high thermal conductivity of BT particles, graphene oxide, and CNTs, which synergistically improved the conductivity. Interestingly, the thermal conductivity of PVDF/CNT/Co-NWs showed a thermal conductivity of ca. 2.8 W m^{-1} K^{-1}, which is highest among the different PVDF-based composite studies here. This increase in thermal conductivity in the composites is due to high thermal conductivity of cobalt nanowires (100 W m^{-1} K^{-1}) and also due to high aspect ratio of the wires. These long nanowires can easily form a network and more conducting pathways resulting in better thermal transfer in the composites. Thus, flexible (Figure 9) and lightweight composites to attenuate EM radiations can be designed by a careful selection of nanoparticles.

CONCLUSIONS

In this study, three key properties were targeted, namely, enhanced dielectric constant, magnetic permeability, and electrical conductivity to design flexible and lightweight PVDF-based composites for EMI shielding. To accomplish this, two unique materials were developed, namely, GO sheets

covalently grafted on to BT nanoparticles and cobalt nanowires. By grafting GO on to a ferroelectric phase (BT), the dielectric constant of the composites could be enhanced significantly in striking contrast to the neat polymer. These nanoparticles in combination with CNTs showed high electrical conductivity and significant attenuation of EM radiations both in the X-band and the K_u-band frequency. The PVDF/CNT/BT−GO and PVDF/CNT/Co-NWs composites exhibited percentage absorption of ca. 63% and 60%, respectively, which is significantly higher than the PVDF/CNT composites. Moreover, the SE was observed to be highest for PVDF/CNT/Co-NWs composites. In addition, PVDF/CNT/BT−GO and PVDF/CNT/Co-NWs composites showed enhanced thermal conductivity in striking contrast to neat PVDF. This study opens new avenues to design flexible and lightweight EMI shielding materials by a careful selection of functional nanoparticles.

AUTHOR INFORMATION

Corresponding Author

*E-mail: sbose@materials.iisc.ernet.in (S.B.). Phone: +91-80-22933407.

Notes

The authors declare no competing financial interest.

ACKNOWLEDGMENTS

The authors like to acknowledge DAE-BRNS, India, for the financial support. C. Srivastava acknowledges the financial support from the IISc-JATP grant.

REFERENCES

(1) Aalto, S.; Haarala, C.; Brück, A.; Sipilä, H.; Hämäläinen, H.; Rinne, J. O. Mobile Phone Affects Cerebral Blood Flow in Humans. *J. Cereb. Blood Flow Metab.* **2006**, *26*, 885−890.

(2) Haarala, C.; Aalto, S.; Hautzel, H.; Julkunen, L.; Rinne, J. O.; Laine, M.; Krause, B.; Hämäläinen, H. Effects of a 902 MHz Mobile Phone on Cerebral Blood Flow in Humans: A Pet Study. *Neuroreport* **2003**, *14*, 2019−2023.

(3) Hockanson, D. M.; Drewniak, J. L.; Hubing, T. H.; Van Doren, T. P.; Sha, F.; Wilhelm, M. J. Investigation of Fundamental EMI Source Mechanisms Driving Common-Mode Radiation from Printed Circuit Boards with Attached Cables. *IEEE Trans. Electromagn. Compat.* **1996**, *38*, 557−566.

(4) Sudo, T.; Sasaki, H.; Masuda, N.; Drewniak, J. L. Electromagnetic Interference (EMI) of System-on-Package (SOP). *IEEE Trans. Adv. Pack.* **2004**, *27*, 304−314.

(5) Du, F.; Fischer, J. E.; Winey, K. I. Effect of Nanotube Alignment on Percolation Conductivity in Carbon Nanotube/Polymer Composites. *Phys. Rev. B* **2005**, *72*, 121404.

(6) Bauhofer, W.; Kovacs, J. A Review and Analysis of Electrical Percolation in Carbon Nanotube Polymer Composites. *Compos. Sci. Technol.* **2009**, *69*, 1486.

(7) Stankovich, S.; Dikin, D. A.; Dommett, G. H.; Kohlhaas, K. M.; Zimney, E. J.; Stach, E. A.; Piner, R. D.; Nguyen, S. T.; Ruoff, R. S. Graphene-Based Composite Materials. *Nature* **2006**, *442*, 282−286.

(8) Bigg, D. M. Mechanical, Thermal, and Electrical Properties of Metal Fiber-Filled Polymer Composites. *Polym. Eng. Sci.* **1979**, *19*, 1188−1192.

(9) Manuel Stephan, A.; Nahm, K. Review on Composite Polymer Electrolytes for Lithium Batteries. *Polymer* **2006**, *47*, 5952−5964.

(10) Chung, D. Electromagnetic Interference Shielding Effectiveness of Carbon Materials. *Carbon* **2001**, *39*, 279−285.

(11) Rohini, R.; Bose, S. Electromagnetic Interference Shielding Materials Derived from Gelation of Multiwall Carbon Nanotubes in Polystyrene/Poly(methyl methacrylate) Blends. *ACS Appl. Mater. Interfaces* **2014**, *6*, 11302−11310.

(12) Al-Saleh, M.; Sundararaj, U. A Review of Vapor Grown Carbon Nanofiber/Polymer Conductive Composites. *Carbon* **2009**, *47*, 2.

(13) Pawar, S. P.; Pattabhi, K.; Bose, S. Assessing the Critical Concentration of Nh2 Terminal Groups on the Surface of MWNTs Towards Chain Scission of PC in PC/SAN Blends: Effect on Dispersion, Electrical Conductivity and Emi Shielding. *RSC Adv.* **2014**, *4*, 18842−18852.

(14) Glatkowski, P.; Mack, P.; Conroy, J. L.; Piche, J. W.; Winsor, P. Electromagnetic Shielding Composite Comprising Nanotubes. U.S. Patent 12,142,623, May 21, 2009.

(15) Bose, S.; Bhattacharyya, A. R.; Khare, R. A.; Kulkarni, A. R.; Pötschke, P. Specific Interactions and Reactive Coupling Induced Dispersion of Multiwall Carbon Nanotubes in Co Continuous Polyamide6/Ionomer Blends. *Macromol. Symp.* **2008**, *263*, 11−20.

(16) Sharma, M.; Sharma, S.; Abraham, J.; Thomas, S.; Madras, G.; Bose, S. Flexible EMI Shielding Materials Derived by Melt Blending PVDF and Ionic Liquid Modified MWNTs. *Mater. Res. Express* **2014**, *1*, 035003.

(17) Pant, H. C.; Patra, M. K.; Verma, A.; Vadera, S. R.; Kumar, N. Study of the Dielectric Properties of Barium Titanate−Polymer Composites. *Acta Mater.* **2006**, *54*, 3163−3169.

(18) Abbas, S.; Chandra, M.; Verma, A.; Chatterjee, R.; Goel, T. Complex Permittivity and Microwave Absorption Properties of a Composite Dielectric Absorber. *Composites, Part A* **2006**, *37*, 2148−2154.

(19) Joseph, N.; Singh, S. K.; Sirugudu, R. K.; Murthy, V. R. K.; Ananthakumar, S.; Sebastian, M. T. Effect of Silver Incorporation into PVDF-Barium Titanate Composites for Emi Shielding Applications. *Mater. Res. Bull.* **2013**, *48*, 1681−1687.

(20) Shui, X.; Chung, D. Nickel Filament Polymer-Matrix Composites with Low Surface Impedance and High Electromagnetic Interference Shielding Effectiveness. *J. Electron. Mater.* **1997**, *26*, 928−934.

(21) Nina, J.; Sebastian, M. Electromagnetic Interference Shielding Nature of PVDF-Carbonyl Iron Composites. *Mater. Lett.* **2013**, *90*, 64−67.

(22) Kim, S. W.; Yoon, Y.; Lee, S.; Kim, G.; Kim, Y. B.; Chun, Y. Y.; Lee, K. Electromagnetic Shielding Properties of Soft Magnetic Powder−Polymer Composite Films for the Application to Suppress Noise in the Radio Frequency Range. *J. Magn. Magn. Mater.* **2007**, *316*, 472−474.

(23) Feng, C.; Liu, X.; Sun, Y.; Jin, C.; Lv, Y. Enhanced Microwave Absorption of Flower-Like FeNi@C Nanocomposites by Dual Dielectric Relaxation and Multiple Magnetic Resonance. *RSC Adv.* **2014**, *4*, 22710−22715.

(24) Al-Saleh, M. H.; Gelves, G. A.; Sundararaj, U. Copper Nanowire/Polystyrene Nanocomposites: Lower Percolation Threshold and Higher EMI Shielding. *Composites, Part A* **2011**, *42*, 92−97.

(25) Bose, S.; Raghu, H.; Mahanwar, P. Mica Reinforced Nylon-6: Effect of Coupling Agents on Mechanical, Thermal, and Dielectric Properties. *J. Appl. Polym. Sci.* **2006**, *100*, 4074−4081.

(26) Bose, S.; Mahanwar, P. A. Effects of Titanate Coupling Agent on the Properties of Mica-Reinforced Nylon-6 Composites. *Polym. Eng. Sci.* **2005**, *45*, 1479−1486.

(27) Xavier, P.; Sharma, K.; Elayaraja, K.; Vasu, K.; Sood, A.; Bose, S. Reduced Graphene Oxide Induced Phase Miscibility in Polystyrene−Poly (Vinyl Methyl Ether) Blends. *RSC Adv.* **2014**, *4*, 12376−12387.

(28) Li, Y.; Huang, X.; Hu, Z.; Jiang, P.; Li, S.; Tanaka, T. Large Dielectric Constant and High Thermal Conductivity in Poly(Vinylidene Fluoride)/Barium Titanate/Silicon Carbide Three-Phase Nanocomposites. *ACS Appl. Mater. Interfaces* **2011**, *3*, 4396−4403.

(29) Srivastava, A.; Singh, R.; Sampson, K.; Singh, V.; Ramanujan, R. Templated Assembly of Magnetic Cobalt Nanowire Arrays. *Metall. Mater. Trans. A* **2007**, *38*, 717−724.

(30) Maurice, J. L.; Imhoff, D.; Etienne, P.; Durand, O.; Dubois, S.; Piraux, L.; George, J. M.; Galtier, P.; Fert, A. Microstructure of Magnetic Metallic Superlattices Grown by Electrodeposition in Membrane Nanopores. *J. Magn. Magn. Mater.* **1998**, *184*, 1−18.

(31) Kirkpatrick, S. Percolation and Conduction. *Rev. Mod. Phys.* **1973**, *45*, 574.
(32) Bao, S.; Liang, G.; Tjong, S. C. Effect of Mechanical Stretching on Electrical Conductivity and Positive Temperature Coefficient Characteristics of Poly (Vinylidene Fluoride)/Carbon Nanofiber Composites Prepared by Non-Solvent Precipitation. *Carbon* **2011**, *49*, 1758−1768.
(33) Psarras, G. C. Hopping Conductivity in Polymer Matrix−Metal Particles Composites. *Composites, Part A* **2006**, *37*, 1545−1553.
(34) Guskos, N.; Anagnostakis, E.; Likodimos, V.; Bodziony, T.; Typek, J.; Maryniak, M.; Narkiewicz, U.; Kucharewicz, I.; Waplak, S. Ferromagnetic Resonance and Ac Conductivity of a Polymer Composite of Fe_3O_4 and Fe_3C Nanoparticles Dispersed in a Graphite Matrix. *J. Appl. Phys.* **2005**, *97*, 024304.
(35) Yan, L.; Wang, J.; Han, X.; Ren, Y.; Liu, Q.; Li, F. Enhanced Microwave Absorption of Fe Nanoflakes after Coating with SiO_2 Nanoshell. *Nanotechnology* **2010**, *21*, 095708.
(36) Eswaraiah, V.; Sankaranarayanan, V.; Ramaprabhu, S. Functionalized Graphene−PVDF Foam Composites for EMI Shielding. *Macromol. Mater. Eng.* **2011**, *296*, 894−898.
(37) Eswaraiah, V.; Sankaranarayanan, V.; Ramaprabhu, S. Inorganic Nanotubes Reinforced Polyvinylidene Fluoride Composites as Low-Cost Electromagnetic Interference Shielding Materials. *Nanoscale Res. Lett.* **2011**, *6*, 1−11.
(38) Lee, B.; Woo, W.; Park, H.; Hahm, H.; Wu, J.; Kim, M. Influence of Aspect Ratio and Skin Effect on EMI Shielding of Coating Materials Fabricated with Carbon Nanofiber/PVDF. *J. Mater. Sci.* **2002**, *37*, 1839−1843.
(39) Arranz-Andrés, J.; Pérez, E.; Cerrada, M. Hybrids Based on Poly (Vinylidene Fluoride) and Cu Nanoparticles: Characterization and EMI Shielding. *Eur. Polym. J.* **2012**, *48*, 1160−1168.
(40) Li, B.-W.; Shen, Y.; Yue, Z.-X.; Nan, C.-W. Enhanced Microwave Absorption in Nickel/Hexagonal-Ferrite/Polymer Composites. *Appl. Phys. Lett.* **2006**, *89*, 132504.
(41) Han, Z.; Fina, A. Thermal Conductivity of Carbon Nanotubes and Their Polymer Nanocomposites: A Review. *Prog. Polym. Sci.* **2011**, *36*, 914−944.
(42) Ye, C. M.; Shentu, B. Q.; Weng, Z. X. Thermal Conductivity of High Density Polyethylene Filled with Graphite. *J. Appl. Polym. Sci.* **2006**, *101*, 3806−3810.
(43) Zhi, C.; Bando, Y.; Terao, T.; Tang, C.; Kuwahara, H.; Golberg, D. Towards Thermoconductive, Electrically Insulating Polymeric Composites with Boron Nitride Nanotubes as Fillers. *Adv. Funct. Mater.* **2009**, *19*, 1857−1862.
(44) Sui, G.; Jana, S.; Zhong, W.; Fuqua, M.; Ulven, C. Dielectric Properties and Conductivity of Carbon Nanofiber/Semi-Crystalline Polymer Composites. *Acta Mater.* **2008**, *56*, 2381−2388.
(45) Elgafy, A.; Lafdi, K. Effect of Carbon Nanofiber Additives on Thermal Behavior of Phase Change Materials. *Carbon* **2005**, *43*, 3067−3074.
(46) Shou, Q. L.; Cheng, J. P.; Fang, J. H.; Lu, F. H.; Zhao, J. J.; Tao, X. Y.; Liu, F.; Zhang, X. B. Thermal Conductivity of Poly Vinylidene Fluoride Composites Filled with Expanded Graphite and Carbon Nanotubes. *J. Appl. Polym. Sci.* **2013**, *127*, 1697−1702.